

BBA 42527

## Oriented purple-membrane films as a probe for studies of the mechanism of bacteriorhodopsin functioning. II. Photoelectric processes

Alexander A. Kononenko <sup>a</sup>, Evgenii P. Lukashev <sup>a</sup>, Sergei K. Chamorovsky <sup>a</sup>,  
Alexander V. Maximychev <sup>b</sup>, Sergei F. Timashev <sup>b</sup>, Lina N. Chekulaeva <sup>c</sup>,  
Andrew B. Rubin <sup>a</sup> and Vladimir Z. Paschenko <sup>a</sup>

<sup>a</sup> Department of Biology, Lomonosov University of Moscow, Moscow, <sup>b</sup> L. Ya. Karpov Institute of Physics and Chemistry, Moscow and <sup>c</sup> Institute of Biological Physics, USSR Academy of Sciences, Pushchino, Moscow Region (U.S.S.R.)

(Received 29 October 1986)

Key words: Purple membrane; Bacteriorhodopsin; Oriented film; Photopotential; Dark potential difference

Photoelectric processes have been investigated in dry orderly oriented preparations of purple membranes from *Halobacterium halobium* under both continuous light and flash excitation. An electrophoretic sedimentation on Al, Cu, Fe, Ni, Pt and SnO<sub>2</sub> substrates was used to obtain orderly oriented purple-membrane films. The photoelectric response of the purple-membrane film is the sum of a light-induced 'displacement' current and a constant steady-state current, the proportion between the two depending upon the chemical nature of the electrodes and humidity of the film. With a high humidity, the steady-state photocurrent is correlated with the reactivity of the cathode metal (toward H<sup>+</sup>) reduction reaction. A correlation is found to exist between the kinetics of photopotential rise and decay and formation and decay of the K<sub>630</sub> and M<sub>412</sub> intermediates of the bacteriorhodopsin photocycle at temperatures ranging from 293 to 83 K, indicating the electrogenic nature of these intermediates. In purple-membrane films deposited on an SnO<sub>2</sub> substrate, a correlation exists between the 'dark' potential and electron work function of the second electrode.

### Introduction

The proton-transport activity of the native bacteriorhodopsin of cellular membranes in the halophilic bacterium *Halobacterium halobium* and the role of bacteriorhodopsin in the cell energetics have been demonstrated by Danon and Stoeckenius [1]. The electrogenic function of bacteriorhodopsin induced by light has been investigated in many studies [1–14,21] using various modeling systems. Vesicles reconstructed with bacteriorhodopsin sheets were used to study the proton-transport activity of bacteriorhodopsin [2–4]. The photoelectric activity of bacteriorhodopsin was first

recorded directly in Ref. 5 by measuring the potential difference across a planar phospholipid membrane modified with bacteriorhodopsin. More stable systems can be obtained by using collodium films, instead of bilayer lipid membranes [6,7], or using a porous filter impregnated with a lipid solution [8,9]. These systems were employed to investigate the fast photoelectric responses of bacteriorhodopsin to a laser flash [6,7]. In a later investigation, the fast components of the photocurrent were recorded in a system in which bacteriorhodopsin sheets were adsorbed on a bilayer lipid membrane [10]. Bacteriorhodopsin sheets deposited on a thin teflon film were used to investigate capacitive currents induced by light pulse excitation [11,12]. Electric potentials were recorded in purple membrane suspension using short

Correspondence: A.A. Kononenko, Department of Biology, Lomonosov University of Moscow, Moscow 119899, U.S.S.R.

voltage pulses for polarization before laser flash [13].

In the above mentioned modelling systems, the bacteriorhodopsin preparation is in contact with the aqueous phase, and measurements are made through electrodes submerged in the electrolyte. There are, however, systems in which electrodes are in direct contact with the bacteriorhodopsin. In an investigation reported in Ref. 14, the fast photoelectric processes were observed by using metal electrodes built in a purple-membrane suspension frozen under applied external electric field. With such a system, it is possible to investigate the kinetics of bacteriorhodopsin-generated photocurrents at fairly low temperatures. Another 'solid state' sample is a multilayer purple-membrane film: a dried suspension of bacteriorhodopsin sheets interposed between transparent, metallic or semiconducting electrodes [15–17]. The procedure of preparing such purple-membrane films was described in Ref. 18, the first work of this series, in which the effect of external electric field on the dark state and photocycle of bacteriorhodopsin was investigated. Samples of this type can also be used to study the inverse problem: light-induced electric processes in bacteriorhodopsin. The studied sample is an electrode system  $C_1$ /bacteriorhodopsin film/ $C_2$  (one electrode being transparent to visible light) across which a voltage can be generated by light.

Using the orientation procedure described in our previous work, it is possible to obtain preparations with bacteriorhodopsin sheets oriented in a single common direction. One can assume that in an orderly oriented bacteriorhodopsin preparation the photoelectric activity is significantly enhanced owing to the absence of the mutual compensation of the photocurrents which takes place in samples with randomly oriented purple membranes. The availability of bacteriorhodopsin preparations with enhanced photoelectric activity would make possible more profound investigations of phenomena responsible for the formation of photocurrents in the bacteriorhodopsin preparation.

In the present work, oriented purple-membrane films were obtained by electrophoretic sedimentation of a purple-membrane suspension on the surface of Al, Cu, Fe, Ni, Pt and  $\text{SnO}_2$ . The photoelectric processes in the purple-membrane

films were investigated at the temperature range 293–83 K both under continuous light and flash excitation. The photoelectric response of the purple-membrane film is the sum of the 'displacement' current and the constant steady-state current component, the proportion between the two depending upon the chemical nature and humidity of the preparation. At high humidity, the amount of steady-state current is correlated with the reactivity of the electrode material in the  $\text{H}^+$  reduction reaction. A similarity in the behavior patterns was found to exist between the rise and decay kinetics of the photopotential and the formation and decay of  $K_{630}$  and  $M_{412}$ , the intermediates of the bacteriorhodopsin photocycle. A correlation was also observed between the work function of the electron in the electrode material and the 'dark' potential of the system containing a purple-membrane film.

## Methods and Materials

Samples were prepared from an aqueous suspensions of purple membranes of *Halobacterium halobium* (strains  $R_1M_1$  and 353-P). Purple membranes were isolated by the method of Oesterhelt and Stoerkenius [19] with a modification of the last stage. Purple membranes obtained by centrifugation in a sucrose gradient were passed through a G-50 sephadex (large grains) column equilibrated with distilled water. This allowed one to fully purify the preparation from sucrose and obtain a uniform preparation devoid of aggregates.

Where no specific orientation was required, 0.02 ml suspension containing 6–7 mg protein per ml, pH 6.5–6.8, was deposited on the substrate plate. A glass plate,  $35 \times 15 \times 1.5$  mm in dimension, coated with an aluminium layer sprayed in vacuo (70% light transmissivity) served as a substrate. A droplet of suspension, spread over an area of  $0.3 \text{ cm}^2$ , was dried in vacuo (13.3 Pa) for 15–20 min. An average optical density of the obtained samples was 0.4 at 560 nm. Using thermal vacuum spraying, a thin aluminium layer was deposited upon the dried purple-membrane film. In some experiments rubbing contracts, made of different metals, were attached instead of using coating. The use of this procedure does not affect the results.

The procedure of orienting purple membranes was described in detail in our previous work [18]. Briefly, it is as follows. After the preliminary deionization, a purple-membrane suspension containing about 15 mg protein/ml was placed between planar electrodes and a permanent electric field of  $30\text{--}50\text{ V}\cdot\text{cm}^{-1}$  was applied for 0.5–3 min. This initiates an orderly electrophoretic sedimentation of bacteriorhodopsin sheets upon the anode. The area of the obtained purple-membrane film is about  $0.5\text{ cm}^2$ ; its optical density is 1.5–2. The oriented purple-membrane films were sedimented on glass plates coated with a tin dioxide layer. In some experiments aluminium, iron, copper and nickel plates were used instead of  $\text{SnO}_2$  as substrates.

Before the experiments each sample was tested for its electric parameters. In randomly oriented preparations, the resistance was measured (with a DC power source) to be typically  $10^{10}\ \Omega$  at room temperature and room humidity. In orderly oriented purple-membrane films, this value was found to vary between  $0.1\cdot 10^{12}$  and  $10\cdot 10^{12}\ \Omega$ . The capacitance, measured at 1 kHz, was  $200 \pm 50\text{ pF}$  for randomly oriented samples and  $20 \pm 10\text{ pF}$  for orderly oriented purple-membrane films. The dif-

ference in the electric parameters between the two types of sample is obviously due to the difference in the sample thickness and specific conductivity of the suspensions used.

Measurements of photo-induced voltages and absorption changes were made on a locally made multi-purpose photobiological test unit. The block diagram of the unit is shown in Fig. 1. A 300 W halogen lamp, coupled to a heat filter, was used as a source of continuous illumination. The light flux was varied within  $200\text{ W}\cdot\text{m}^{-2}$ . Glass, broad-band absorption filters were used to isolate the desired wavelength of actinic light.

For low-temperature experiments, the sample, fixed in a holder of the cryostat (the latter was cooled with liquid nitrogen) was placed in a transparent Dewar flask. The flask was placed in the cuvette chamber of the instrument. To protect the sample from the condensation moisture appearing during the cooling, the substrate, with the purple-membrane film on, was coated with another glass plate and sealed with a Parafilm M. A schematic presentation of the overall sample assembly is given in Fig. 1 (inset). A copper/constantan thermocouple was used to control temperature.

Photopotentials were measured on light-adapted samples (10-min preillumination). An electrometer with an input resistance of  $10^{14}\ \Omega$  was used for steady-state measurements. In some experiments, the samples were shunted with a resistor, varied within 0.1 to  $100\text{ G}\Omega$ .

Laser-flash experiments were performed using 15-ns flashes at 530 nm. The flash energy was 3.5 mJ. A broad-band amplifier with an input resistance of  $10^{11}\ \Omega$  and signal rise time of  $15\text{ V}/\mu\text{s}$  was used in the measuring network of the flash-induced potential.

Photopotential measurements were also made on preparations with different humidity. To have the desired moisture content each purple-membrane film to be tested, with its upper electrode attached to but with no coating glass plate, was kept in an excicator in the vapor of a saturated solution of a selected salt for 48 h to allow the equilibrium to be attained; by using different salts it was possible to obtain different humidity. Where it was not necessary to know the actual moisture content of the preparations, the humidity was varied by placing the samples, for different times,

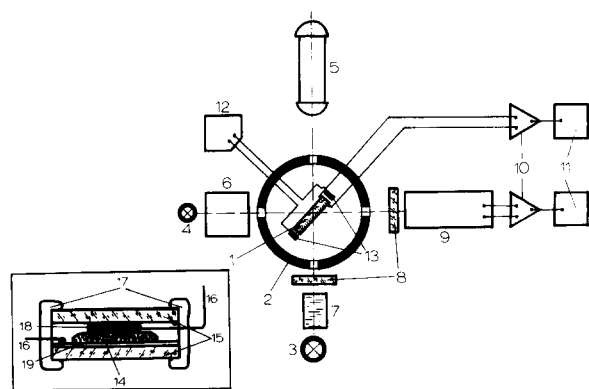


Fig. 1. A schematic diagram of a multi-purpose setup for biological studies: (1) sample under study; (2) cuvette chamber of the cryostat; (3) source of exciting light; (4) source of monitoring light; (5) laser; (6) monochromator; (7) heat filter; (8) cut glass filters; (9) photomultiplier; (10) amplifiers; (11) recorders; (12) polarizing voltage generator; (13) electrodes used to polarize the suspension. Inset: an arrangement of sample 1; (14) film composed of purple membranes; (15) glass plates; (16) metallic conductors; (17) water-proof isolating film; (18) metallic electrode; (19) current-conducting coating layer.

in an air-tight screen-protected chamber in a saturated water vapor. The incubation time, which was varied from 10 min to 2 h, was used as a measure of sample moisture.

When not in use, the samples were stored at room temperature and a relative humidity of 90% to prevent cracking or detaching from the substrate plate.

## Results and Discussion

For the  $C_1$ /bacteriorhodopsin/ $C_2$  electrode system consisting of a film of sedimented purple membranes and current-conducting elements, we shall use the following notation: the substrate that holds bacteriorhodopsin sheets is indicated by  $C_1$ , and the electrode (sprayed or pressed) by  $C_2$ . The  $C_2$  electrode will be termed photopositive, and the substrate photonegative for on the light the potential of  $C_2$  shows rise in the positive direction, in both orderly and randomly oriented bacteriorhodopsin preparations [18].

Control tests were conducted in the preliminary experiment using films of inert materials between the electrodes (methyl cellulose, lipids, etc.) instead of purple membranes, and also films of a purple-membrane suspension at acidic pHs (less than 3) at which bacteriorhodopsin is in an inactive 'blue' state [20]. No photopotential generation was observed in those systems.

### Dark potential

As reported in our previous work [21,22], a potential difference is generated in the dark and persists for a long time in oriented dry films of purple-membrane. Its magnitude at room temperature varies from several millivolts to about 30 mV, depending on the electrode metal. At the present time, no convincing explanation for its generation can be offered. In the  $\text{SnO}_2$ /bacteriorhodopsin/Me and Me/bacteriorhodopsin/ $\text{SnO}_2$  systems, the metallic electrode (Me) is negatively charged in the dark. With increasing the humidity (under non-equilibrium conditions) the 'dark' potential shows rise by more than one order of magnitude. In symmetric systems,  $\text{SnO}_2$ /bacteriorhodopsin/ $\text{SnO}_2$  or Al/bacteriorhodopsin/Al, the potential difference is nearly zero in the dark.

With high humidity the potential difference in

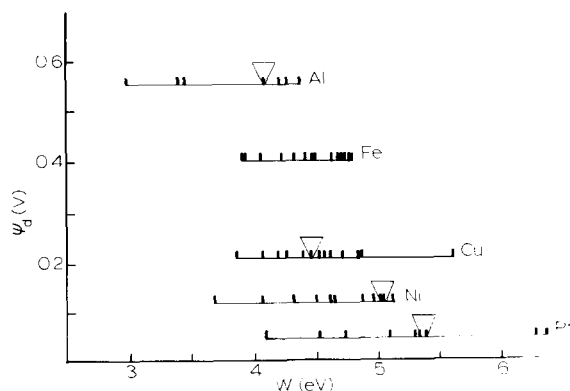


Fig. 2. Correlation between work function of electron  $W$  and dark potential in a  $\text{SnO}_2$ /bacteriorhodopsin/Me system. The values of  $W$  used are from Ref. 23 triangular symbols show the most probable values of  $W$  [23].

the  $\text{SnO}_2$ /bacteriorhodopsin/Me systems and the electron work function ( $W$ ) are antipate in character (Fig. 2). The experimentally measured parameter  $W$  is highly sensitive to the surface state of the metal and depends largely on the measurement method used. For this reason, the difference in the  $W$  value of the same metal as measured by various authors may be as much as 1.0–1.5 eV [23]. Despite that there is some uncertainty in the  $W$  value, it can be concluded from the data of Fig. 2 that the lesser the electron work function of metal, the higher the dark potential difference. The potential measured under such conditions is either stationary or of corrosion origin [24]. Perhaps oxidation of some structural groups and reduction of others take place, while water is being involved in the process. The observed correlation can be related to the dependence of the corrosive processes in metal on the Fermi level.

### *The influence of purple-membrane orientation, humidity of the preparation and chemical nature of the electrode on photoresponses of purple-membrane films*

The orientation of purple membranes by electrophoretic sedimentation results in a significant (two-orders-of-magnitude) rise of the steady-state photopotential generated by light in air-dried purple-membrane films. Typical values of the photopotentials observed in orderly and in randomly

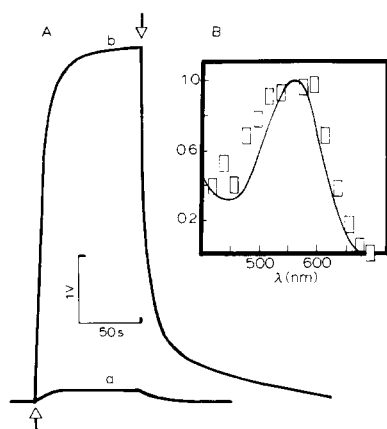


Fig. 3. (A) Kinetics of photopotential generated by purple membrane films: (a) a typical curve for a preparation with non-oriented purple membranes; (b) a typical curve for a film with orderly oriented purple membranes;  $\uparrow$  and  $\downarrow$ , lights on and off, respectively. (B) The absorption spectrum of a purple-membrane film (solid line) and the photopotential action spectrum, normalized to the 570 nm peak.

oriented preparations are shown in Fig. 3. The action spectrum for the photopotential (Fig. 3, inset) is analogous to the absorption spectrum of a dry purple-membrane film. Owing to the significantly larger photoelectric signals in the orderly oriented purple-membrane preparations, it is possible to investigate phenomena responsible for the formation of the photocurrent and to analyse the kinetics of the fast photoelectric processes in the purple-membrane film.

Two main photoresponses of the purple-membrane film can be distinguished (Fig. 4): (a) a momentary signal generated immediately after the application of light (curves b); and (b) a steady-state potential attaining its constant level several seconds after the onset of the illumination (curve a). A combination of the two signals was commonly observed (curve c). There is a view [25] that in dry bacteriorhodopsin sheet preparations, in contrast to native purple membranes, illumination causes only a local displacement of the protons from the equilibrium position (particularly,  $H^+$  transfer from the Schiff base to a neighboring proton-binding group), which is followed by the return of  $H^+$  to the initial binding site. In support of this view is the behavior pattern of the photopotential kinetics in the dry purple-membrane films. In Fig. 4, curve b is a typical transition

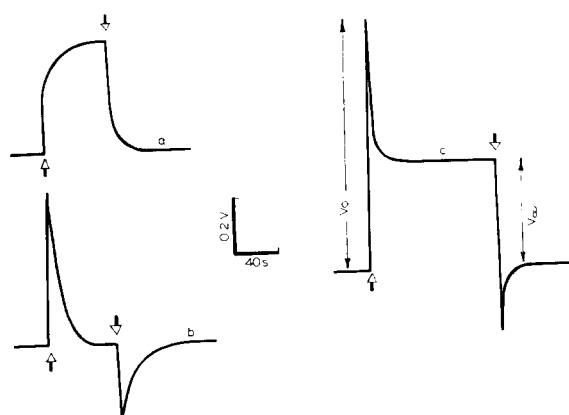


Fig. 4. Kinetics of potential changes in  $SnO_2$ /bacteriorhodopsin/Me systems under continuous illumination.  $\uparrow$  and  $\downarrow$ , lights on and off, respectively. (a)  $SnO_2$ /bacteriorhodopsin/Fe system after 1-h humidification; load resistance  $R_1 = 6.8 \text{ G}\Omega$ ; (b)  $SnO_2$ /bacteriorhodopsin/ $SnO_2$  system with room humidity;  $R_1 = 1 \text{ G}\Omega$ ; (c)  $SnO_2$ /bacteriorhodopsin/Pt system after 10-min humidification,  $R_1 = 1 \text{ G}\Omega$ .

characteristic for the displacement of bound charges. In addition to the current associated with the displacement of protons, the photoresponse of the purple-membrane preparation has a permanent current component (curves a and c) whose magnitude depends on the load resistance, preparation humidity and chemical nature of the material in contact with the purple-membrane film.

In a purple-membrane preparation with a higher humidity, the contribution of the permanent component to the electrogenesis of bacteriorhodopsin is greater. The current associated with the charges displacement remain without change. The dependence of the steady-state photopotential on the incubation time is shown in Fig. 5 for  $SnO_2$ /bacteriorhodopsin/Fe and  $SnO_2$ /bacteriorhodopsin/Pt samples.

To investigate the effect of the substrate material on the photopotential, we prepared oriented purple-membrane films deposited on aluminum, iron, copper and nickel plates. With  $SnO_2$  used as a photo-positive electrode, the steady-state photopotential is about 10 mV. No noticeable difference in the values of  $V_\infty$  was observed for different substrate materials. The replacement of  $SnO_2$  for Al gives rise to the steady-state photopotential by approx. one order of magnitude. In the order of increasing the pho-

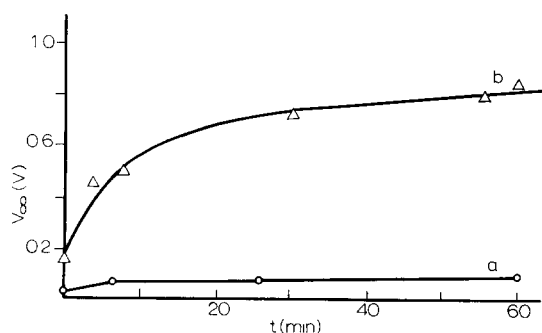


Fig. 5. The dependence of the steady-state photopotential in a  $\text{SnO}_2$ /bacteriorhodopsin/Fe (a) and  $\text{SnO}_2$ /bacteriorhodopsin/Pt (b) system on the time of sample incubation in a saturated water-vapor atmosphere. Shunt resistor, 1 G $\Omega$ .

topotential, the materials used as a substrate in a Me/bacteriorhodopsin/Al system are  $\text{SnO}_2 > \text{Ni} \sim \text{Cu} \sim \text{Fe} > \text{Al}$ . After the electrophoretic sedimentation on  $\text{SnO}_2$ , the purple-membrane films with room humidity exhibited photopotentials of 0.2–0.35 V (with a shunt of 6.8 G $\Omega$  connected across the sample). At this humidity,  $V_\infty$  shows no dependence on the chemical nature of the positive electrode. After 15-min humidification, under 100% humidity, the purple-membrane film showed rise in the steady-state potential to 1 V in the  $\text{SnO}_2$ /bacteriorhodopsin/Ni and  $\text{SnO}_2$ /bacteriorhodopsin/Pt systems. The humidification appeared to be without effect on the steady-state photopotential in samples with an Al or Cu positive electrode. In a symmetric  $\text{SnO}_2$ /bacteriorhodopsin/ $\text{SnO}_2$  system, the photopotential was measured to be not greater than 1.0–1.5 mV. For  $\text{SnO}_2$ /bacteriorhodopsin/Me system, the metals in the order of increasing the photopotential are:  $\text{Pt} \sim \text{Ni} > \text{Fe} > \text{Al} \sim \text{Cu} \gg \text{SnO}_2$ . The highest photocurrent (to 15.5 nA  $\cdot \text{cm}^{-2}$ ) was observed in a humidified  $\text{SnO}_2$ /bacteriorhodopsin/Pt sample shunted with a  $10^8 \Omega$  resistor.

#### Electrochemical processes at the interfaces of the sample assembly

The current flowing in the external measuring network depends on the functional state of the bacteriorhodopsin sheets and on the property of the electrode material to act as an electron donor or acceptor in oxidation-reduction reactions. Suppose that only one reaction occurs at each elec-

trode and both equilibria are shifted toward the 'forward' reaction. Then, for the forward current on the positive electrode,  $i_+$ , and backward current on the negative electrode,  $i_-$ , we have

$$i_\pm = j_0^\pm \exp(\mp \alpha_\pm e \eta_\pm / k_B T) \quad (1)$$

where  $j_0^\pm$  are the exchange currents which characterize the kinetic behavior of the electrochemical process occurring in the electrode made of a given material;  $\alpha_\pm$  are the transfer coefficients, which for most electrode processes differ little from 0.5 [26];  $\eta_\pm$  are the electrode overvoltage;  $e$  is an elementary charge;  $k_B$  is Boltzmann's constant;  $T$  is the temperature. In the steady state,  $i_+ = i_-$ . Assuming that  $\alpha_+ = \alpha_- = \alpha$ , we have:

$$\ln j_0^+ - \ln j_0^- = \alpha e (\eta_+ + \eta_-) / k_B T \quad (2)$$

The quantity  $\eta_+ + \eta_-$  on the right-hand side of Eqn. 2 is the steady-state potential difference  $V_\infty$ . It follows from Eqn. 2 that there is a linear relation between  $V_\infty$  and the logarithm of the exchange current on the electrode.

From the sign of the photopotential generated by the bacteriorhodopsin proton pump and the character of the changes in the bacteriorhodopsin photoresponses with changes in the sample humidity we can postulate that the dominant process at the positive electrode is the reduction of  $\text{H}^+$  ions. In fact, values of the steady-state photopotential  $V_\infty$  in the  $\text{SnO}_2$ /bacteriorhodopsin/Me system (Fig. 6) are correlated with values of  $\ln j_0$  for hydrogen reduction at the cathode [26]. The insensitivity of  $V_\infty$  to the material of the positive electrode in the dry purple-membrane preparations suggests that the photocurrents are limited by the bacteriorhodopsin properties, for instance, due to the slowing of the bacteriorhodopsin photocycle at low humidity [27]. The acceleration of the cycle in preparations with high moisture contents results in that the processes at the bacteriorhodopsin/Me interface become a limiting step.

The transport of  $\text{H}^+$  toward the  $\text{C}_2$  electrode is to be accompanied by coupled reactions at the photonegative electrode, occurring with the involvement of  $\text{OH}^-$ . The process involving  $\text{OH}^-$  (particularly, anode oxygen evolution) is known [28] to be accompanied by secondary reactions, which make the investigation of the primary pro-

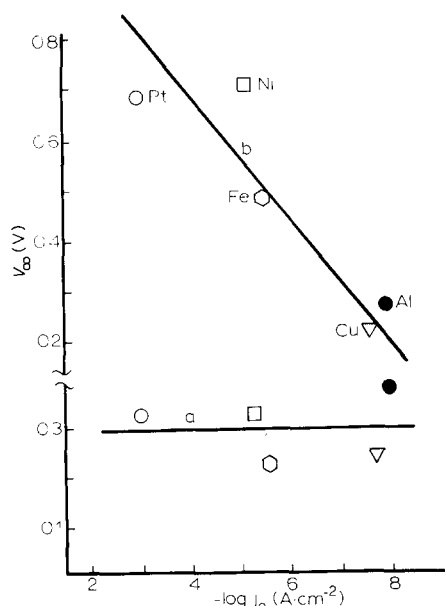


Fig. 6. Relation between steady-state photopotential in a  $\text{SnO}_2$ /bacteriorhodopsin/Me system and exchange-current density in a reaction of cathode  $\text{H}^+$  reduction in an aqueous solution. (a) Air-dried preparation (40% moisture content); (b) samples kept in a saturated water-vapor atmosphere for 30 min.

cess difficult. The formation of oxides strongly affects the oxygen-evolution kinetics; moreover, the structure of the oxide layer also alters in the course of the reaction. A possible oxidation of the anode organic matrix makes the picture even more complicated. Our data show that the steady-state potential in the Me/bacteriorhodopsin/Al system depends little on the substrate material. Probably, the presence of oxides at some stage causes the metals to behave in a common way in the  $\text{HO}^-$ -dependent reactions. No correlation was found to exist between the value of the photopotential  $V_\infty$  and physico-chemical properties of the substrate.

#### *Temperature dependence of the photopotential generated in purple-membrane films under continuous illumination*

The temperature dependence of the photopotential was investigated in Al/bacteriorhodopsin/Al samples. Simultaneous measurements of the electric response and absorption changes of the  $M_{412}$  product under continuous illumination

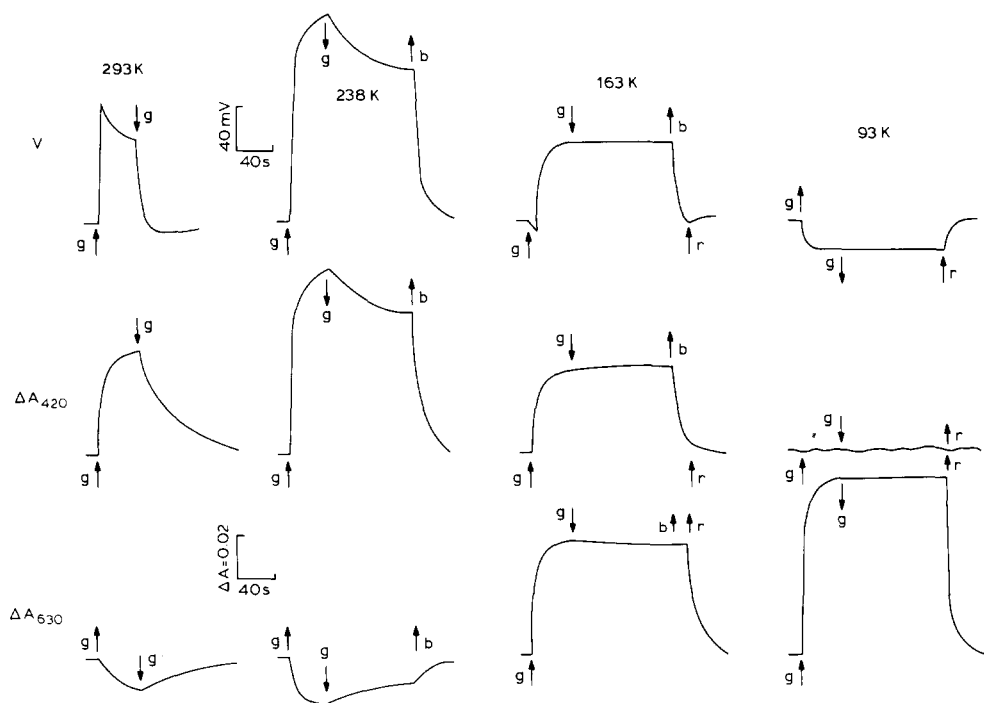


Fig. 7. Kinetics of the photopotential ( $V$ ) and photo-induced absorption changes at 420 nm ( $\Delta A_{420}$ ) and 630 nm ( $\Delta A_{630}$ ) in purple-membrane films at different temperatures.  $\uparrow$  and  $\downarrow$ , lights on and off, respectively; labeling letters adjacent to the arrows stand for green (g), blue (b) and red (r) light.

showed that they have resembling although not fully identical kinetics (Fig. 7). The light curve of the photopotential and absorption changes at 420 nm also appeared to be virtually the same in the behavior pattern.

In the temperature experiments, the photo-induced absorption changes were measured at 420 nm, the absorption band of the  $M_{412}$  intermediate, and at 630 nm, the absorption band of the  $K_{630}$  product of the bacteriorhodopsin photocycle. With lowering the temperature to 263 K, the amplitudes of the steady-state photoelectrical response and 420-nm absorbance show both a marked rise. This is associated with the significant slowing of the dark recovery of the electric potential and  $M_{412}$  formation. The characteristic time of the recovery process increases under these conditions to several minutes. At temperatures from 238 K to 223 K, at which the conversion of  $M_{412}$  into the initial bacteriorhodopsin<sub>570</sub> state is blocked, as demonstrated by Balashov and Lozier and coworkers [29,30], the decay kinetics of the 420-nm absorption changes become irreversible; similar changes are distinct in the decay kinetics of the photopotential, reflecting the stability of a certain bacteriorhodopsin state corresponding to the  $M_{412}$  intermediate. At temperatures to 133 K, the photo-induced formation of the  $M_{412}$  intermediate and the concomitant generation of the photopotential were observed (Fig. 7). Excitation by blue light (which falls within the absorption band of the  $M_{412}$ ), following the removal of green light, affected the bacteriorhodopsin form caused the  $M_{412}$  to decay rapidly and the electric potential to disappear. These observations agree with results reported in Refs. 30 and 31 that excitation with light at wavelengths within the absorption band of the intermediates of the bacteriorhodopsin photocycle stimulates reactions leading to the regeneration of its initial state. Owing to this property of bacteriorhodopsin, it was possible to follow the photopotential kinetics and photo-induced absorption changes in a single sample over the temperature range 293–83 K. The dependence of the photopotential on the spectral content of actinic light at physiological temperatures was investigated in detail in Refs. 32–34. At temperatures below 223 K, we observed a diminution of the steady-state amount of  $M_{412}$  and a lowering of

the photopotential, which are related to the blockage of the bacteriorhodopsin<sub>570</sub>  $\rightarrow$   $M_{412}$  transition [30,31].

The most interesting results were obtained in observing the photopotential kinetics and light-induced absorption changes at low temperatures, from 173 to 83 K. The accumulation of the considerable amount of the  $K_{630}$  batho-intermediate was observed at as low a temperature as 163 K. Significant changes occurred simultaneously in the photopotential kinetics. The electric response to light exposure becomes biphasic, the fast phase being small in amplitude and opposite in sign relative to the steady-state photopotential. The inverse phase becomes a single component of the photopotential at temperatures below 133 K, when the  $K_{630} \rightarrow M_{412}$  transition is fully blocked, and illumination by green light leads to the accumulation of the  $K_{630}$  batho-product in the stable state. The maximum value of the steady-state photopotential at 83 K, which is opposite in sign to that observed at positive temperatures, is commonly below 30–50 mV for the preparations with randomly oriented purple membranes. At low temperatures, the  $K_{630}$  intermediate formed in green light and the corresponding potential persist without change after switching the light off. Red light, which is within the absorption band of the  $K_{630}$ , activates the reversal of the  $K_{630}$  into the initial bacteriorhodopsin form, which is accompanied by the fast disappearance of the electric potential (Fig. 7).

The obtained results agree well with the concept that the formation and decay of the intermediates of the bacteriorhodopsin photocycle are electrogenic in nature; at least, this is true for the  $K_{630}$  and  $M_{412}$ .

#### *Temperature dependence of the fast kinetic phases of the photopotential under light pulse excitation*

The kinetics of the fast components of the photopotential can be investigated in detail by exciting a purple-membrane preparation by a short laser flash wherever only one turnover of the bacteriorhodopsin cycle can be activated. The temperature dependence of the fast components of the photopotential was investigated using oriented purple-membrane films obtained by electrophoretic sedimentation on a nickel electrode in a



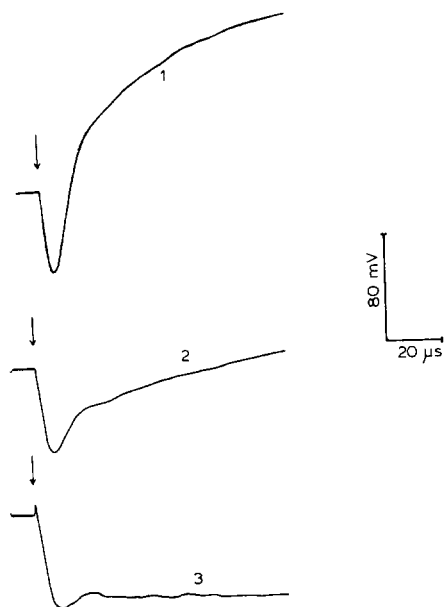


Fig. 8. Kinetic curves of laser-flash-induced potential in orderly oriented purple-membrane films of *H. halobium* at different temperatures. (1) 285 K; (2) 275 K; (3) 165 K.

#### Ni/bacteriorhodopsin/Al electrode system.

Presented in Fig. 8 are kinetic curves for the laser-flash-induced formation of the photopotential in oriented purple-membrane samples at different temperatures. At room temperatures, one first observes the negative phase with the rise time that is shorter than the response time of the recording equipment ( $t_{1/2} \leq 300$  ns). The negative phase is further substituted by changes that are opposite in sign. A kinetic analysis shows that at room temperature these positive changes consist of at least two exponential components with characteristic times of  $t_{1/2} = 2-3$   $\mu$ s and  $t_{1/2} = 15-25$   $\mu$ s. At lower temperatures the kinetics do not change qualitatively. The fast negative phase is kinetically unresolvable to temperatures as low as 113 K. This is in agreement with the observations reported in Ref. 14. It was shown in this investigation using a water-glycerol purple-membrane suspension frozen in electric field that at cryogenic temperatures the negative phase of the laser-flash-induced changes of the photocurrent has fast kinetics with a characteristic time within the time response of the recording equipment ( $t_{1/2} \approx 2-3$   $\mu$ s).

The positive changes at room and low tempera-

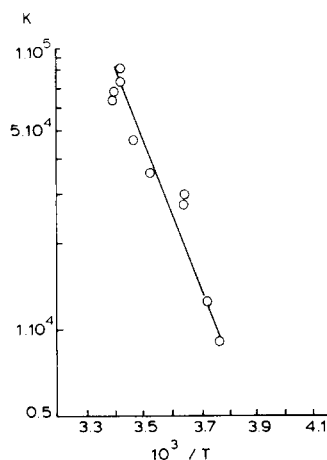


Fig. 9. An Arrhenius plot of the rise kinetics of the second microsecond phase of photopotential as a function of temperature.

tures have two-component kinetics: a 2–3  $\mu$ s component, which is clearly seen in the second and third traces of Fig. 8, and a slower component that slows more with lowering the temperature. An Arrhenius plot of the temperature dependence of this component is shown in Fig. 9. The activation energy for the process is 0.5 eV. The characteristic time of this component is 15–25  $\mu$ s at room temperature, which is nearly equal to the time of the photoinduced formation of the  $M_{412}$  intermediate ( $t_{1/2} \approx 24$   $\mu$ s, Fig. 10). The fact that the  $M_{412}$  formation and the slow microsecond phase of potential generation have nearly the same life-times suggests that this component is related to the formation of  $M_{412}$ , that is, to the deprotonation of the Schiff base of a bacteriorhodopsin molecule [29]. A similar interpretation of the microsecond phase of transmembrane potential gen-

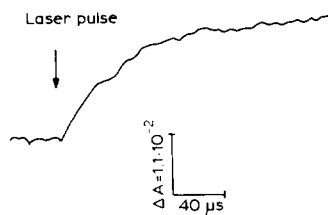


Fig. 10. Kinetics of laser-induced formation of the M intermediate in orderly oriented purple membrane films of *H. halobium*, recorded as absorption changes at 412 nm.

eration of a bacteriorhodopsin molecule was offered in Refs. 6 and 7. In support of this conclusion are nearly the same values of the activation energies of this process (0.5 eV, Fig. 9) and for the photo-induced formation of  $M_{412}$  in an aqueous purple-membrane suspension (0.69 eV) [35].

The origin of the two other stages of electric signal generation is much less clear. One can say for certain that they are associated with the early events of the bacteriorhodopsin conversion. By its kinetic properties, the negative phase can be correlated to  $K_{630}$  formation. That this phase is fast in kinetic behavior and has the large amplitude at cryogenic temperatures suggests that it may be related to the photo-induced shift in the electronic density of a bacteriorhodopsin molecule rather than to the transfer of a heavier charged particle through a rather long distance. It has earlier been postulated in the literature [36] that the primary light energy transformation in bacteriorhodopsin is a shift of the electronic density of the retinal. The kinetics of the fast positive component of photopotential rise at room temperature ( $t_{1/2} = 2\text{--}3\ \mu\text{s}$ ) resemble those of the formation of the L-intermediate absorbing at 540 nm (in an aqueous purple-membrane suspension,  $t_{1/2} = 1\ \mu\text{s}$  [29]). However, at low temperatures the kinetics of the L-formation are much slower [35]. Presumably, this kinetic phase of photopotential reflects the occurrence of light-induced processes other than the formation of the L-intermediate. For instance, absorption changes occurring much faster ( $\tau = 0.5\text{--}0.9\ \mu\text{s}$ ) than the formation of the L-intermediate were observed in Ref. 37 and ascribed to the protonation of the tryptophan residues of a bacteriorhodopsin molecule. Data are available from Raman spectroscopy [38], indicating the occurrence of fast processes in bacteriorhodopsin with rates much higher than the formation of the L-intermediate.

## Conclusion

The potential difference built up in the dark across the substrate plate and electrode contacting the purple-membrane film arises from the corrosive and, possibly, other chemical processes. There is a correlation between the chemical potential of the electrons in the metal and the 'dark' potential

of the  $\text{SnO}_2$ /bacteriorhodopsin/Me system.

The contribution of the current associated with the displacement of protons and the contribution of the steady-state current to the light-induced electric processes in purple-membrane films depend on the moisture content of the preparation and on the chemical nature of the electrode material. At a low humidity, the photocurrents in a purple-membrane film system are limited by the transport properties of bacteriorhodopsin. With the acceleration of the photocycle in a humidified preparation, the processes at the purple-membrane film/electrode interface become a limiting step. The correlation between the magnitude of the photopotential and exchange currents (Fig. 6) suggests that a reduction of  $\text{H}^+$  takes place at the photopositive electrode.

It is found that under continuous illumination at temperatures between 293 and 133 K there is a correspondence between the kinetic characteristics and steady-state values of the photopotential and the steady-state concentration of the  $M_{412}$  intermediate. At temperatures below 163 K, illumination causes an accumulation of the batho-intermediate and a concomitant appearance of a photopotential component opposite in sign to the steady-state photoresponse observed at physiological temperatures. The behavior pattern of the kinetics of the laser-flash-induced photopotential confirms that the formations of the  $M_{412}$  and generation of the photopotential have nearly similar kinetic characteristics. The light-induced electric response of purple-membrane films has a fast negative component which was first observed in Ref. 6. By its kinetic behavior, this component can be correlated to the formation of the  $K_{630}$  batho-product. That the negative phase remains fast ( $t_{1/2} \leq 300\ \text{ns}$ ) even at cryogenic temperatures suggests that the primary events of the bacteriorhodopsin photocycle go concomitant with a significant redistribution of the electronic density at the active center of bacteriorhodopsin [36]. However, the answer to the fundamental question about the nature of the primary events of the bacteriorhodopsin photocycle requires further experimental and theoretical investigations. Data of picosecond-resolved Raman spectroscopy indicate the involvement of the *trans-cis* isomerization of the bacteriorhodopsin retinal in such processes [39].

TABLE I

PHOTOCURRENTS GENERATED BY PREPARATIONS CONTAINING BACTERIORHODOPSIN AND LIGHT-TO-CURRENT CONVERSION FACTORS (RATIO OF SPECIFIC SURFACE ELECTRIC POWER TO LIGHT FLUX DENSITY)

System containing bacteriorhodopsin	Specific resistivity ( $\Omega \cdot \text{cm}^{-2}$ )	Photocurrent density ( $A \cdot \text{cm}^{-2}$ )	Conversion factor	Area ( $\text{cm}^2$ )	References
1 Purple membranes inlaid in planar lipid bilayer	$10^8 - 10^{10}$	$10^{-9}$	$10^{-8} - 10^{-6}$	0.01	5,41
2 Bacteriorhodopsin embedded to proteoliposomes	$2 \cdot 10^{10}$	$10^{-9}$	$2 \cdot 10^{-6}$	0.01	42
3 Bacteriorhodopsin embedded in proteoliposomes attached to a lipid membrane containing ion channels	$10^6$	$4 \cdot 10^{-8}$	$5 \cdot 10^{-8}$	0.01	43
4 Purple membranes in acrylamide gel	$2 \cdot 10^2$	$5 \cdot 10^{-6}$	$5 \cdot 10^{-8}$	7	44
5 Purple membranes attached to an ion-exchange membrane	$10^2$	$10^{-5}$	$2 \cdot 10^{-8}$	15	45
6 Air-dried film of oriented purple membranes with resistor shunt	$10^7$	$1.5 \cdot 10^{-8}$	$2 \cdot 10^{-7}$	0.1	present work

The original purple-membrane preparation used in the present investigation is a sandwich of 1000 membrane monolayers. Orientation causes a significant rise in the photocurrent of the preparation, by more than an order of magnitude. A comparison of our data with the literature data suggests that high photocurrents can be generated by preparations composed of oriented purple membranes with a high degree of ordering and immobilized on membranes with high ion permeability. Table I is an illustration of photocurrents generated by bacteriorhodopsin in different systems and the efficiency of light-current conversion by those systems. Note that with the availability of purple-membrane preparations capable of generating two-order-of-magnitude higher currents it would be possible to compete with preparations containing hydrogenase [40] which are currently under investigation as a photo-source of hydrogen. In contrast to these enzymatic systems, isolated purple membranes are much more stable and less susceptible to detrimental effects.

## References

- 1 Danon, A. and Stoeckenius, W. (1974) *Proc. Natl. Acad. Sci. USA* 71, 1234-1238
- 2 Racker, E. and Stoeckenius, W. (1974) *J. Biol. Chem.* 249, 662-663
- 3 Kaushin, L.P. and Skulachev, V.P. (1974) *FEBS Lett.* 39, 39-42
- 4 Hwang, S.-B. and Stoeckenius, W. (1977) *J. Membrane Biol.* 33, 325-350
- 5 Drachev, L.A., Kaulen, A.D., Ostroumov, S.A. and Skulachev, V.P. (1974) *FEBS Lett.* 39, 43-45
- 6 Drachev, L.A., Kaulen, A.D. and Skulachev, V.P. (1978) *FEBS Lett.* 87, 161-167
- 7 Drachev, L.A., Kaulen, A.D., Khitrina, L.V. and Skulachev, V.P. (1981) *Eur. J. Biochem.* 117, 461-470
- 8 Block, M.C., Hellingwerf, K.J. and Van Dam, K. (1977) *FEBS Lett.* 76, 45-50
- 9 Moran, A., Tal, E. and Nelson, N. (1980) *FEBS Lett.* 110, 62-64
- 10 Fahr, A., Luger, P. and Bamberg, E. (1981) *J. Membr. Biol.* 60, 51-62
- 11 Trissl, H.-W. and Montal, H. (1977) *Nature* 226, 655-657
- 12 Hong, F.T. and Montal, M. (1979) *Biophys. J.* 25, 465-472
- 13 Keszthelyi, L. and Ormos, P. (1980) *FEBS Lett.* 109, 189-193

- 14 Ormos, P., Reinisch, L. and Keszthelyi, L. (1983) *Biochim. Biophys. Acta* 722, 471–479
- 15 Borisevich, G.P., Lukashev, E.P., Kononenko, A.A. and Rubin, A.B. (1979) *Biochim. Biophys. Acta* 546, 177–184
- 16 Lukashev, E.P., Vozary, E., Kononenko, A.A., Rubin, A.B. and Abdulaev, N.G. (1982) *Bioorgan. Khimia* 8, 1173–1179 (in Russian)
- 17 Chamorovsky, S.K., Lukashev, E.P., Kononenko, A.A. and Rubin, A.B. (1983) *Biochim. Biophys. Acta* 725, 403–406
- 18 Kononenko, A.A., Lukashev, E.P., Maximychev, A.V., Chamorovsky, S.K., Rubin, A.B., Timashev, S.F. and Chekulaeva, L.N. (1986) *Biochim. Biophys. Acta* 850, 162–169
- 19 Oesterhelt, D. and Stoekenius, W. (1974) *Methods Enzymol.* 31, 667–678
- 20 Mowery, P.C., Lozier, R.H., Quae-Chae, Tseng, Y.W., Taylor, M. and Stoekenius, W. (1979) *Biochem.* 18, 4100–4107
- 21 Lukashev, E.P., Kononenko, A.A. and Rubin, A.B. (1981) *Biolog. Membrany* 1, 91–98 (in Russian)
- 22 Maximychev, A.B., Lukashev, E.P., Kononenko, A.A., Chekulaeva, L.N. and Timashev, S.F. (1984) *Biolog. Membrany*, 1, 294–304 (in Russian)
- 23 Hodgman, C.D. (ed.), *Handbook of Chemistry and Physics* (1960) The Chemical Rubber Publishing Co., Cleveland, OH
- 24 Gurevich, Yu.Ya. and Pleskov, Yu.V. (1983) *Photochemistry of Semiconductors*, p. 47, Nauka, Moscow
- 25 Hwang, S.-B., Korenbrot, I.I. and Stoekenius, W. (1978) *Biochim. Biophys. Acta* 509, 300–317
- 26 Suhotin, A.M. (ed.) (1981) *Handbook of Electrochemistry*, p. 186, Khimija, Leningrad
- 27 Korenstein, R. and Hess, B. (1977) *Nature* 270, 184–186
- 28 Fetter, K. (1967) *Electrochemical Kinetiks*, p. 856, Khimija, Moscow
- 29 Lozier, R.H., Bogomolni, R.A. and Stoekenius, W. (1975) *Biophys. J.* 15, 955–962
- 30 Balashov, S.P. and Litvin, F.F. (1981) *Biofizika* 26, 557–570 (in Russian)
- 31 Becher, B. and Ebrey, T. *Biophys. J.* (1977) 17, 185–191
- 32 Hwang, S.-B., Korenbrot, J.I. and Stoekenius, W. (1977) in *Bioenergetics of Membranes* (Packer, L. et al., eds.), pp. 137–147, Elsevier/North-Holland Biomedical Press, Amsterdam
- 33 Nagy, K. (1978) *Biochem. Biophys. Res. Commun.* 81, 383–390
- 34 Dancshazy, Zs. and Karvaly, B. (1976) *FEBS Lett.* 72, 136–138
- 35 Zubov, B.V., Sulimov, N.A., Chernavskaya, N.M., Chernavskiy, D.S. and Chizsov, N.V. (1982) *Biofizika* 27, 357–361 (in Russian)
- 36 Warshel, A. (1978) *Proc. Natl. Acad. Sci. USA* 75, 2558–2562
- 37 Kuschmitz, D. and Hess, B. (1982) *FEBS Lett.* 138, 137–140
- 38 Braiman, M. and Mathies, R. (1982) *Proc. Natl. Acad. Sci. USA* 79, 403–407
- 39 Hsien, Ch.-Lu and El-Sayed, M.A. (1983) *Photochem. Photobiol.* 38, 83
- 40 Yaropolov, A.I., Karyakin, A.A., Gogotov, I.N., Zorina, N.A., Varfolomeev, S.D. and Berezin, I.V. (1984) *Dokl. Acad. Nauk SSSR* 274, 1434–1437 (in Russian)
- 41 Herrmann, T.R. and Rayfield, G.W. (1976) *Biochim. Biophys. Acta* 443, 623–638
- 42 Drachev, L.A., Frolov, V.N., Kaulen, A.D., Liberman, E.A., Ostroumov, S.A., Plakunova, V.G., Semenov, A.Yu. and Skulachev, V.P. (1976) *J. Biol. Chem.* 251, 7059–7065
- 43 Severina, I.I. (1983) *Biokhimija* 48, 1522–1529 (in Russian)
- 44 Eisenbach, M., Weissmann, C., Tanny, G. and Caplan, S.R. (1977) *FEBS Lett.* 81, 77–80
- 45 Singh, K., Korenstein, R., Lebedeva, H. and Caplan, S.R. (1980) *Biophys. J.* 31, 393–402